On the Role of Interconnection Directionality in the Quadratic Performance of Double-Integrator Networks

H. Giray Oral, Enrique Mallada, *Senior Member, IEEE*, and Dennice Gayme, *Senior Member, IEEE*

***Abstract*— This note provides a quantitative and qualitative evaluation of the role of interconnection directionality in a general class of quadratic performance metrics for double-integrator networks. We first develop an analysis framework that can be used to evaluate the quadratic performance metrics of networks defined over a general class of directed graphs. A comparison between systems whose directed graph Laplacians are normal and their undirected counterparts unveils an interplay between the interconnection directionality and the control strategy that determines network performance. We show that directionality can significantly degrade performance; however well-designed feedback can exploit directionality to mitigate this degradation or even improve performance.**

***Index Terms*— Directed Graph, $\mathcal{H}_2$, $\mathcal{L}_2$ norm, Performance**

I. Introduction

Conditions for reaching consensus -achieving a synchronized steady state- have been widely studied for networked dynamical systems, see e.g. [1]–[3]. A related and equally important question is how the system performs in its effort to restore and/or maintain synchrony in the face of disturbances. This synchronization performance can be interpreted as a measure of efficiency or robustness, and has been evaluated, for example, in terms of the lack of coherence or the degree of disorder in first order (single-integrator) [4]–[10] and second order (double-integrator) [6], [11]–[16] consensus networks. Related robustness metrics for power systems (e.g. transient real power losses or phase/frequency incoherency) have been assessed in transmission and inverter-based networks [17]–[25].

The synchronization effort, which can be formulated within a general class of quadratic performance metrics, is evaluated in closed-form for undirected networks in e.g., [6], [11], [18], [21], [24], [26]–[30]. Related work explores directed interconnection topologies including spatially invariant [31] and nearest-neighbor type interactions [15]; as well as systems with normal [5], [7], [16] and diagonalizable [32] weighted Laplacian matrices. More general directed graph topologies have also been considered and bounds on quadratic metrics are obtained in [33]. The notion of effective graph resistance [34] has been extended to directed graphs [35], [36], which can enable the evaluation of the lack of coherence in first order consensus networks over certain directed topologies. These works have made progress towards evaluating the quadratic performance metrics of directed networks, however a precise understanding of the role of the interconnection directionality has yet to be developed.

In this note, we first define a general class of quadratic performance metrics in terms of the $\mathcal{L}_2$ norm (signal energy) of the system output when the networked system is subjected to impulse disturbances at each node. This class of metrics can, for example, be used to quantify the effort required to maintain a vehicle formation equilibrium (e.g. coordination of position and velocity). Adopting the terminology from vehicle networks, the metrics are defined in terms of either the position or the velocity states of agents. We develop a unifying analysis framework that can be used to compute these performance metrics for high-order integrator networks defined over *arbitrary* directed graphs; under the mild topological assumption that the graph contains at least one globally reachable node. This framework applies to a broad range of systems, but here we focus on the well-studied class defined by double-integrator networks. In particular, we exploit our framework to isolate the underlying system properties that enable the analysis of the role of directionality in the performance of double-integrator networks for the special case where the interconnection structure leads to a normal weighted graph Laplacian. In the vehicle coordination example (e.g., spatially invariant formations [6], [12]), this directionality can emerge from limiting the number of sensors per vehicle.

The role of directionality is evaluated through a comparative analysis of the performance of directed graphs and their ‘equivalent undirected graphs’ [36], which we refer to as their ‘undirected counterparts’. We define this undirected counterpart as the Hermitian part of the normal weighted Laplacian matrix. Our results indicate that the effect of directionality on performance can be characterized by the spectral structures of the weighted graph Laplacian and output matrices. More precisely, we demonstrate that the presence of observable Laplacian eigenvalues with nonzero imaginary part (i.e. the observability of modes associated with directed paths) can significantly degrade both position and velocity based performance compared to the systems with the undirected topology. Nevertheless, this degradation can be eliminated for velocity-based metrics using absolute position feedback. On the other hand, for position-based metrics a proper combination of relative position and velocity feedback can, not only mitigate this degradation, but also lead to improved performance over the systems with the undirected topology. These results demonstrate previously undiscovered properties of the class of directed networks emitting normal weighted Laplacians, which have implications for their control.

The remainder of this note is organized as follows. In Section II the system models and the performance metrics are introduced. In Section III, we present a decomposition of the closed-loop dynamics and discuss the stability of the input-output system. In Section IV, we develop our general analysis framework. In Section V, we provide the closed-form solutions for the performance metrics of the class of double-integrator networks emitting normal weighted directed graph Laplacians, which are used in Section VI to evaluate the role of interconnection directionality in performance. Section VII concludes the note.

II. System Models and Performance Metrics

A. Double-Integrator Networks

Consider n dynamical systems that communicate over a weighted directed graph $\mathcal{G} = \{\mathcal{N}, \mathcal{E}, \mathcal{W}\}$. Here, $\mathcal{N} = \{1, ..., n\}$ is the set of nodes and $\mathcal{E} = \{(i, j) \mid i, j \in \mathcal{N}, i \neq j\}$ is the set of edges with weights $\mathcal{W} = \{b_{ij} > 0 \mid (i, j) \in \mathcal{E}\}$. In the following $b_{ij} = 0$ if and only if $(i, j) \notin \mathcal{E}$. The following assumption is imposed throughout this note.

Assumption 1. *$\mathcal{G}$ has at least one globally reachable node.*

H. G. Oral and D. F. Gayme are with the Dept. of Mechanical Engineering, E. Mallada is with the Dept. of Electrical and Computer Engineering at The Johns Hopkins University, Baltimore, MD, USA, 21218, {giray, dennice, mallada}@jhu.edu. Support by the NSF (CNS 1544771, EPCN 1711188) is gratefully acknowledged.

We consider double-integrator nodal dynamics of the form $\ddot{x}_i + k_d\dot{x}_i + k_p x_i = u_i + \mathrm{w}_i$, where $u_i = -\gamma_p \sum_{j=1}^{n} b_{ij}(x_i - x_j) - \gamma_d \sum_{j=1}^{n} b_{ij}(\dot{x}_i - \dot{x}_j)$ $\forall i \in \mathcal{N}$. Here, $k_p, k_d, \gamma_p, \gamma_d \geq 0$, denote the control gains (which can be interpreted as augmented stiffness and damping coefficients in vehicle networks) and w_i denotes a disturbance to the i^{th} system. Defining $\mathbf{v} := \dot{\mathbf{x}}$, the double-integrator dynamics can be expressed in matrix form as

$$\begin{bmatrix} \dot{\mathbf{x}} \\ \dot{\mathbf{v}} \end{bmatrix} = \begin{bmatrix} 0 & I \\ -k_p I - \gamma_p L & -k_d I - \gamma_d L \end{bmatrix} \begin{bmatrix} \mathbf{x} \\ \mathbf{v} \end{bmatrix} + \begin{bmatrix} 0 \\ I \end{bmatrix} \mathbf{w}, \tag{1}$$

where L denotes the weighted graph Laplacian matrix given by $[L]_{ii} = \sum_{j=1}^{n} b_{ij}$, and $[L]_{ij} = -b_{ij}$ if $i \neq j$, $\forall i, j \in \mathcal{N}$.

A necessary condition for (1) to reach consensus without disturbance (i.e., $\mathbf{w} = 0$) is that at least one of (k_p, γ_p) and at least one of (k_d, γ_d) are non-zero (which follows from [3, Theorem 1], see [16, Lemma 3] for a self-contained proof). To ensure that this condition is met, we impose the following assumption throughout the note.

Assumption 2. *System* (1) *has feedback in both state variables (position and velocity), i.e. at least one of* (k_p, γ_p) *and at least one of* (k_d, γ_d) *are non-zero.*

B. Performance Metrics

Performance metrics that are quadratic in the state variables are widely used to evaluate system robustness to disturbances. In this note we focus on the analysis of such metrics through a general output norm based approach in order to gain insight into how communication directionality affects performance in systems of the form in (1).

For $C \in \mathbb{R}^{q \times n}$, the performance output

$$\mathbf{y} = C\mathbf{x} \tag{2}$$

will be used to quantify the performance metrics related to the position state $\mathbf{x}$. Similarly, we employ the performance output

$$\mathbf{y} = C\mathbf{v}, \tag{3}$$

to quantify performance metrics related to the velocity state $\mathbf{v}$.

We are interested in performance metrics of the form

$$P = \|\mathbf{y}\|_{\mathcal{L}_2}^2 = \int_0^\infty \mathbf{y}(t)^* \mathbf{y}(t) dt, \tag{4}$$

i.e. metrics formulated as the signal energy of a performance output $\mathbf{y}(t)$, when the system is subject to an impulse input

$$\mathbf{w}(t) = \mathbf{w}_0 \delta(t) \tag{5}$$

with an arbitrary direction vector $\mathbf{w}_0 \in \mathbb{R}^n$. Similar metrics appear in [28] for networks over undirected graphs. Denoting the impulse response function from $\mathbf{w}(t)$ to $\mathbf{y}(t)$ by $T(t)$, the performance output can be written as $\mathbf{y}(t) = \int_0^t T(t-\tau)\mathbf{w}(\tau)d\tau$. Combining this equation with (5) and substituting into (4) gives

$$P = \int_0^\infty \mathbf{w}_0^* T(t)^* T(t) \mathbf{w}_0 dt. \tag{6}$$

We only study input-output stable systems $T(t)$, ensuring finiteness of (6). Stability conditions for $T(t)$ are discussed in Section III-A.

We now show that for a special case of the impulse input (5), the performance metric (6) can be computed using the $\mathcal{H}_2$ norm of $T(t)$. This relationship, which is standard in the literature [17], will be used in the upcoming sections.

Proposition 1. *Consider a strictly proper and stable system* $G(t)$ *from* $\mathbf{w}$ *to* $\mathbf{y}$*, a random impulse input* (5) *with* $E[\mathbf{w}_0\mathbf{w}_0^*] = I$ *and zero initial condition. Then* $\|G\|_{\mathcal{H}_2}^2 = E\left[\|\mathbf{y}\|_{\mathcal{L}_2}^2\right]$.

III. Block-diagonalization of the Closed-loop Dynamics

In this section, we express the dynamics (1) in the frequency domain using an approach based on [28]. This procedure facilitates the stability analysis in Subsection III-A and provides the decomposition of the network topological characteristics and nodal dynamics upon which our general analysis framework in Section IV relies.

The framework, depicted in Figure 1, describes identical systems $g(s)$ receiving feedback that depends on an arbitrary transfer function $f(s)$ and the weighted graph Laplacian L emitted by the network interconnection. Assuming that $\mathbf{x}(0) = \mathbf{v}(0) = 0$, the closed-loop system from the input $\mathbf{w}$ to the position state $\mathbf{x}$ is given by $[(g(s)^{-1}I + f(s)L]\mathbf{x}(s) = \mathbf{w}(s)$, which leads to

$$\mathbf{x}(s) = [(I + g(s)f(s)L]^{-1} g(s)\mathbf{w}(s) =: H_{\mathbf{xw}}(s)\mathbf{w}(s), \tag{7}$$

where $H_{\mathbf{xw}}(s)$ denotes the transfer function from the input $\mathbf{w}$ to the position state $\mathbf{x}$.

L can be decomposed as $L = RJR^{-1}$, where $R \in \mathbb{C}^{n\times n}$ is invertible and $J \in \mathbb{C}^{n\times n}$ is in Jordan Canonical Form (JCF). This decomposition transforms (7) into

$$\mathbf{x}(s) = R\,[(I + g(s)f(s)J]^{-1} g(s)R^{-1}\mathbf{w}(s),$$

as shown in the block diagram in Figure 2. Defining $\tilde{\mathbf{x}} := R^{-1}\mathbf{x}$ and $\tilde{\mathbf{w}} := R^{-1}\mathbf{w}$, the transfer function from $\tilde{\mathbf{w}}$ to $\tilde{\mathbf{x}}$ is

$$H_{\tilde{\mathbf{x}}\tilde{\mathbf{w}}}(s) = [(I + g(s)f(s)J]^{-1} g(s), \tag{8}$$

where the following relationship holds

$$H_{\mathbf{xw}} = RH_{\tilde{\mathbf{x}}\tilde{\mathbf{w}}}R^{-1}. \tag{9}$$

J is composed of Jordan blocks J_k associated with the eigenvalues $\lambda_k \in \mathbb{C}$ of L for $k = 1, \ldots, m$:

$$J = \mathrm{blockdiag}\,(J_k)_{1\leq k\leq m}, \tag{10}$$

where $J_k \in \mathbb{C}^{n_k\times n_k}$ and $\sum_{k=1}^{m} n_k = n$. Since L is a Laplacian matrix, $L\mathbf{1} = \mathbf{0}$ with $\mathbf{1}$ denoting the vector of all ones, therefore $J_1 = \lambda_1 = 0$. Also $\mathrm{Re}\,[\lambda_k] > 0$ for $k = 2, \ldots, m$ due to the fact that $\mathcal{G}$ has a globally reachable node [37, Theorem 7.4]. So (8) can be written as

$$H_{\tilde{\mathbf{x}}\tilde{\mathbf{w}}}(s) = \mathrm{blockdiag}\left(H_{\tilde{\mathbf{x}}_k\tilde{\mathbf{w}}_k}(s)\right)_{1\leq k\leq m}, \tag{11}$$

where

$$H_{\tilde{\mathbf{x}}_k\tilde{\mathbf{w}}_k}(s) = [(I + g(s)f(s)J_k]^{-1} g(s). \tag{12}$$

Here, the vectors $\tilde{\mathbf{x}}_k = [\tilde{x}_{d_k+1}, \ldots, \tilde{x}_{d_k+n_k}]^\mathsf{T}$ and $\tilde{\mathbf{w}}_k = [\tilde{w}_{d_k+1}, \ldots, \tilde{w}_{d_k+n_k}]^\mathsf{T}$ respectively denote the position state and the input to the associated subsystem, with $d_1 = 0$ and $d_k = \sum_{i=1}^{k-1} n_i$ for $k = 2, \ldots, m$. An equivalent representation of the transfer function in (12) is given by the block diagram in Figure 3. The following lemma describes the form of the transfer function in (12) which will be used to compute the performance metric (6).

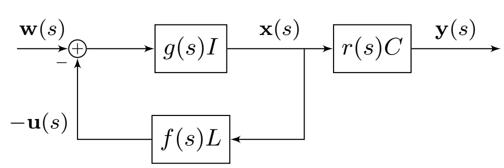

Fig. 1: Block diagram of the closed-loop system $T(s)$ from the disturbance input $\mathbf{w}(s)$ to the performance output $\mathbf{y}(s)$ and the closed-loop system $H_{\mathbf{xw}}(s)$ from $\mathbf{w}(s)$ to the position state $\mathbf{x}(s)$. The performance output $\mathbf{y}(s)$ is given by (2) if $r(s) = 1$ and by (3) if $r(s) = s$.

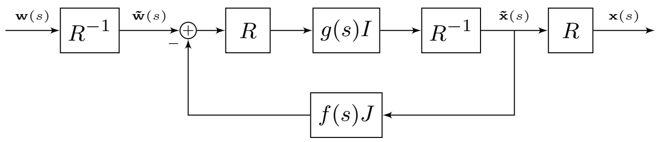

Fig. 2: Application of a change of basis given by the Jordan decomposition $L = RJR^{-1}$ to the closed-loop system $H_{\mathbf{xw}}(s)$. The feedback loop gives the closed-loop system $H_{\tilde{\mathbf{x}}\tilde{\mathbf{w}}}(s)$.

Lemma 1. *$H_{\tilde{\mathbf{x}}_k\tilde{\mathbf{w}}_k}(s)$ in (12) is an upper triangular Toeplitz matrix given by*

$$H_{\tilde{\mathbf{x}}_k\tilde{\mathbf{w}}_k}(s) = \frac{1}{f(s)}\begin{bmatrix} h_k(s) & \dots & (-1)^{n_k-1}h_k(s)^{n_k} \\ & \ddots & \vdots \\ & & h_k(s)\end{bmatrix},$$

where $h_k(s) = \frac{g(s)f(s)}{1+\lambda_k g(s)f(s)}$.

Proof. See [38], [39] for a proof. □

Remark 1. *The closed-loop transfer function in Lemma 1 holds for arbitrary open-loop and feedback transfer functions $g(s)$ and $f(s)$, hence it applies to a general class of networked dynamical systems.*

We next apply Lemma 1 to the double-integrator network (1).

Corollary 1. *Consider the double-integrator network* (1)*. Then, $H_{\tilde{\mathbf{x}}_k\tilde{\mathbf{w}}_k}(s)$ in (12) is the upper triangular Toeplitz matrix*

$$H_{\tilde{\mathbf{x}}_k\tilde{\mathbf{w}}_k}(s) = \frac{1}{\gamma_p + s\gamma_d}\begin{bmatrix} h_k(s) & \dots & (-1)^{n_k-1}h_k(s)^{n_k} \\ & \ddots & \vdots \\ & & h_k(s)\end{bmatrix},$$

where $h_k(s) = \frac{\gamma_p+s\gamma_d}{s^2+(k_d+\gamma_d\lambda_k)s+k_p+\gamma_p\lambda_k}$.

Proof. See [38], [39] for a proof. □

The transfer function from the input $\mathbf{w}$ to the velocity state $\mathbf{v}$ is $H_{\mathbf{vw}}(s) := sH_{\mathbf{xw}}(s)$ since $\mathbf{v}(s) = s\mathbf{x}(s) = sH_{\mathbf{xw}}(s)\mathbf{w}(s)$. Then, the closed-loop transfer function $T(s)$ from the input $\mathbf{w}$ to the output $\mathbf{y}$ can be written as

$$T(s) = Cr(s)H_{\mathbf{xw}}(s), \tag{13}$$

using the notation in Figure 1 and specifying $r(s)$ such that

$$T(s) = \begin{cases} CH_{\mathbf{xw}}(s), & r(s) = 1 \quad (14a) \\ CH_{\mathbf{vw}}(s), & r(s) = s\ . \quad (14b)\end{cases}$$

The cases (14a) and (14b) correspond to the outputs (2) and (3), respectively. We next provide necessary and sufficient conditions for the input-output stability of (14a) and (14b), which ensure the finiteness of the performance metric (6).

A. Input-Output Stability

We now state necessary and sufficient conditions for the input-output stability of (14a) and (14b). The following assumption will be imposed throughout the note to exclude the unstable consensus mode of the Laplacian from the performance output.

Assumption 3. *The output matrix C satisfies $C\mathbf{1} = \mathbf{0}$.*

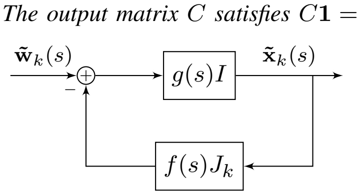

Fig. 3: Block diagram of each subsystem $H_{\tilde{\mathbf{x}}_k\tilde{\mathbf{w}}_k}$ for $k = 1, \dots, m$.

First, we apply the change of basis in (9) to the closed-loop system (13). Since $L\mathbf{1} = \mathbf{0}$, we can apply the partitioning

$$R = \begin{bmatrix}\alpha\mathbf{1} & \tilde{R}\end{bmatrix} \text{ and } R^{-1} = \begin{bmatrix}\mathbf{q}_1 & \tilde{Q}^*\end{bmatrix}^*, \tag{15}$$

where $\alpha \in \mathbb{C}$, $\mathbf{q}_1^* \in \mathbb{C}^{1\times n}$ is the left eigenvector of $\lambda_1 = 0$, $\tilde{R} \in \mathbb{C}^{n\times n-1}$ and $\tilde{Q} \in \mathbb{C}^{n-1\times n}$. Substituting (9), (11) and (15) into (13) we obtain

$$T(s) = C\left(\alpha r(s)H_{\tilde{\mathbf{x}}_1\tilde{\mathbf{w}}_1}(s)\mathbf{1}\mathbf{q}_1^* + \tilde{R}\tilde{H}(s)\tilde{Q}\right) = C\tilde{R}\tilde{H}(s)\tilde{Q}, \tag{16}$$

where

$$\tilde{H}(s) = \text{blockdiag}\,(\tilde{H}_k(s)) := r(s)\,\text{blockdiag}\left(H_{\tilde{\mathbf{x}}_k\tilde{\mathbf{w}}_k}(s)\right), \tag{17}$$

for $k = 2, \dots, m$ and we have used Assumption 3 and the fact that $H_{\tilde{\mathbf{x}}_1\tilde{\mathbf{w}}_1}(s)$ is a scalar. We can partition $\tilde{R}$ in (15) as

$$\tilde{R} = \begin{bmatrix}\tilde{R}_2 & \dots & \tilde{R}_m\end{bmatrix}, \tag{18}$$

which is in a form that conforms to (10). Then the columns of $\tilde{R}_k \in \mathbb{C}^{n\times n_k}$ are the right generalized eigenvectors associated with the Jordan block J_k in (10) for $k = 2, \dots, m$. This partitioning leads to the following useful definition.

Definition 1. *The set of observable indices $\mathcal{N}_{obsv}$ is given by*

$$\mathcal{N}_{obsv} = \left\{k \in \{2, \dots, m\} \mid C\tilde{R}_k \neq 0\right\}. \tag{19}$$

As we show next for the double-integrator network (1), stability of the observable modes is necessary and sufficient for the input-output stability of the system T given by (14a) or (14b). We assume L is diagonalizable in Proposition 2, which is sufficient for the analysis in Section VI.

Proposition 2. *Consider the double-integrator network* (1) *and suppose that L is diagonalizable and assumptions 1, 2 and 3 hold. The system T given by* (14a) *or* (14b) *is input-output stable if and only if*

$$s^2 + (k_d + \gamma_d\lambda_k)s + k_p + \gamma_p\lambda_k = 0 \tag{20}$$

has solutions that satisfy $\text{Re}(s) < 0$ for all $k \in \mathcal{N}_{obsv}$.

Proof. See [38], [39] for a proof. □

The stability condition in Proposition 2 can be restated as two inequalities that solely and simultaneously depend on the weighted Laplacian eigenvalues associated with the observable modes and the control gains. This restatement helps characterize the allowable gain values for given topology and performance metric of interest.

Proposition 3. *Consider the double-integrator network* (1) *and suppose that L is diagonalizable and assumptions 1, 2 and 3 hold. The system T given by* (14a) *or* (14b) *is input-output stable if and only if*

$$\alpha_k\phi_k^2 + \beta_k\xi_k\phi_k - \beta_k^2 > 0 \text{ and } \phi_k > 0, \quad k \in \mathcal{N}_{obsv}, \tag{21}$$

where $\alpha_k = k_p + \gamma_p\,\text{Re}[\lambda_k]$, $\phi_k = k_d + \gamma_d\,\text{Re}[\lambda_k]$, $\beta_k = \gamma_p\,\text{Im}[\lambda_k]$ and $\xi_k = \gamma_d\,\text{Im}[\lambda_k]$.

Proof. Applying [3, Lemma 2] to Proposition 2 gives the result. □

Propositions 2 and 3 generalize the necessary and sufficient conditions for second order consensus [3, Theorem 1] to input-output stability conditions, which are required for the performance evaluation in Section VI. We next introduce our framework for analyzing the performance of directed networks.

IV. A General Analysis Framework

In this section, we use the block-diagonalization procedure outlined in Section III to develop an analysis framework for the performance of networks over arbitrary directed graphs that have at least one globally reachable node. This framework is applicable to a general class of nodal dynamics and will be used in the upcoming sections for our analysis. Throughout the discussion we use both time and frequency domain representations, which simplifies the analysis.

First, we simplify (6) using the block-diagonal form of (11) and show that performance can be quantified as a linear combination of scalar integrals. These integrals can be interpreted as $\mathcal{L}_2$ scalar products of the elements of the closed-loop impulse response function matrix blocks $H_{\tilde{\mathbf{x}}_k\tilde{\mathbf{w}}_k}(t)$ and $H_{\tilde{\mathbf{v}}_k\tilde{\mathbf{w}}_k}(t)$.

Combining (6) and (16), the performance metric in (6) can be written as

$$P = \int_0^\infty \mathbf{w}_0^* \tilde{Q}^* \tilde{H}(t)^* \tilde{N} \tilde{H}(t) \tilde{Q} \mathbf{w}_0 dt, \tag{22}$$

where $\tilde{N} = \tilde{R}^* C^* C \tilde{R}$ and $\tilde{H}$ is of the form in (17) with

$$\tilde{H}_k(s) = \begin{bmatrix} \tilde{h}_{11}^{(k)}(s) & \dots & \tilde{h}_{1,n_k}^{(k)}(s) \\ & \ddots & \vdots \\ & & \tilde{h}_{n_k,n_k}^{(k)}(s) \end{bmatrix} \tag{23}$$

for $k = 2, \dots, m$. The upper triangular form of (23) is given in Lemma 1. Since

$$M := C^* C \tag{24}$$

is a symmetric matrix, it is unitarily diagonalizable, i.e.

$$M = \Theta W \Theta^*, \quad W = \operatorname{diag}(\mu_i)_{1 \le i \le n} \in \mathbb{R}^{n \times n}, \quad \text{and} \quad \Theta\Theta^* = I,$$

therefore $\tilde{N} = \tilde{R}^* \Theta W \Theta^* \tilde{R}$. Using Assumption 3 and assuming without loss of generality that $\mu_1 = 0$ is associated with the eigenvector $\boldsymbol{\theta}_1 = \frac{1}{\sqrt{n}}\mathbf{1}$, we can state $\tilde{N}$ element-wise as

$$(\tilde{N})_{\eta-1,\kappa-1} = \sum_{l=2}^{n} \langle \boldsymbol{\theta}_l, \mathbf{r}_\eta \rangle \langle \mathbf{r}_\kappa, \boldsymbol{\theta}_l \rangle \mu_l =: \nu_{\eta,\kappa} \tag{25}$$

for $\eta, \kappa = 2, \dots, n$, where $\langle \boldsymbol{\theta}_l, \mathbf{r}_\eta \rangle = \mathbf{r}_\eta^* \boldsymbol{\theta}_l$, $\mathbf{r}_\kappa$ and $\boldsymbol{\theta}_l$ respectively denote the columns κ and l of $\tilde{R}$ and Θ.

Using this notation, (22) can be written in terms of the scalar products between the elements of $\tilde{H}_k(t)$, which are given by the element-wise inverse Laplace transforms of (23).

Theorem 1. *The performance metric P in (22) is given by*

$$P = \operatorname{tr}(\Sigma_Q \Psi), \tag{26}$$

where

$$\Sigma_Q = \tilde{Q}\Sigma_0\tilde{Q}^*, \; \Sigma_0 = \mathbf{w}_0\mathbf{w}_0^*, \tag{27}$$

and the matrix Ψ is partitioned as $\Psi = [\Psi_{kl}]_{2 \le k,l \le m}$.

Furthermore, the entry (q, b) of the matrix Ψ_{kl} for $k, l = 2, \dots, m$ is given by

$$[\Psi_{kl}]_{qb} = \sum_{p=1}^{q} \sum_{a=1}^{b} \nu_{d_k+p, d_l+a} \left\langle \tilde{h}_{ab}^{(l)}(t), \tilde{h}_{pq}^{(k)}(t) \right\rangle_{\mathcal{L}_2}, \tag{28}$$

where

$$\left\langle \tilde{h}_{ab}^{(l)}(t), \tilde{h}_{pq}^{(k)}(t) \right\rangle_{\mathcal{L}_2} = \int_0^\infty \overline{\tilde{h}_{pq}^{(k)}(t)} \tilde{h}_{ab}^{(l)}(t) dt. \tag{29}$$

Here the indices $q = 1, \dots, n_k$ and $b = 1, \dots, n_l$ are determined by the Jordan block sizes n_k and n_l. Terms of the form in (25) appear in the summand of (28) and their indices take values larger than the sum of the previous Jordan block sizes, namely $d_k = \sum_{i=1}^{k-1} n_i$ and $d_l = \sum_{i=1}^{l-1} n_i$.

Remark 2. *For the special case in which L is diagonalizable each Jordan block is a scalar, i.e. $n_k = 1$, and (28) leads to*

$$\Psi_{kl} = \nu_{kl} \left\langle \tilde{h}^{(l)}(t), \tilde{h}^{(k)}(t) \right\rangle_{\mathcal{L}_2}.$$

Here we dropped the subscripts of $\tilde{h}_{pq}^{(k)}$ for simplicity. The case with diagonalizable L was studied in [28], [29] and Theorem 1 provides a generalization to the case of arbitrary Jordan block size n_k for $k = 2, \dots, m$.

Proof of Theorem 1. Taking the trace of both sides of (22) and using the permutation property of the trace yields $P = \operatorname{tr}\left(\tilde{Q}\mathbf{w}_0\mathbf{w}_0^*\tilde{Q}^*\Psi\right)$, where $\Psi(t) = \int_0^\infty \tilde{H}(t)^*\tilde{N}\tilde{H}(t)dt$. Partitioning $\tilde{N}$ conformally so that its (k,l) block is given by $\tilde{N}_{kl}$, one can write

$$\Psi_{kl} = \int_0^\infty \tilde{H}_k(t)^* \tilde{N}_{kl} \tilde{H}_l(t) dt, \tag{30}$$

for $k, l = 2, \dots, m$. Direct multiplication of the matrices in the integral argument and interchanging the order of integration with the summation gives the desired result. ☐

Remark 3. *Since $\tilde{N} = \tilde{N}^*$, i.e. $\tilde{N}_{kl} = \tilde{N}_{lk}^*$, (30) leads to $\Psi_{kl} = \Psi_{lk}^*$, therefore Ψ is Hermitian. The fact that Σ_Q in (27) is also Hermitian leads to $\operatorname{tr}(\Sigma_Q\Psi) = \operatorname{tr}\left[(\Sigma_Q\Psi)^*\right] = \overline{\operatorname{tr}(\Sigma_Q\Psi)}$, which verifies that P in (26) is real as expected.*

As Theorem 1 indicates, (26) can be expressed in closed-form if the integral in (29) can be evaluated. Theorem 1 therefore provides a general framework for the computation of the performance metrics, which can be utilized by first deriving time-domain realizations of the transfer functions $\tilde{h}_{pq}^{(k)}(s)$ in (23), and then using these realizations to evaluate the integral in (29). We refer the reader to [38], [39] for the computation of closed-form solutions to general quadratic performance metrics of single and double-integrator networks over arbitrary directed graphs that have at least one globally reachable node. We next focus on systems emitting normal Laplacian matrices to illustrate a specific application of our general framework.

V. Closed-form Solutions with Normal Laplacians

In this section, we provide the closed-form solutions of the performance metrics for the class of systems whose interconnection topologies emit normal weighted Laplacian matrices, using our general framework. We will then use these closed-form solutions to investigate the role of interconnection directionality in Section VI.

First recall Definition 1, which introduced the set of observable indices $\mathcal{N}_{obsv}$ in (19). If L is normal, it is diagonalizable, and we can re-state this set as

$$\mathcal{N}_{obsv} = \{k \in \{2, \dots, n\} \mid C\mathbf{r}_k \neq 0\},$$

recalling that $\mathbf{r}_k$ denotes the k^{th} right eigenvector of L as defined in (15). We now present two lemmas that will be useful in proving the upcoming results.

Lemma 2. *For $k \in \{2, \dots, n\}$, the eigenvalue-eigenvector pair $(\mu_k, \boldsymbol{\theta}_k)$ of M in (24) satisfies $\mu_k = 0$ if and only if $C\boldsymbol{\theta}_k = 0$.*

Proof. See [38], [39] for a proof. ☐

Lemma 3. *Suppose that L is normal. For $k \in \{2, \dots, n\}$, ν_{kk} in (25) satisfies*

1) *$\nu_{kk} = 0$ if and only if $k \notin \mathcal{N}_{obsv}$.*
2) *$\nu_{kk} > 0$ if and only if $k \in \mathcal{N}_{obsv}$.*

Proof. See [38], [39] for a proof. ☐

We now provide the closed-form solutions to the general quadratic performance metrics for the class of double-integrator systems that emit normal Laplacian matrices. This result generalizes the result given in [16, Corollary 2] to position and velocity based performance metrics with arbitrary output matrices.

Lemma 4 (Double-Integrator, Normal Laplacian)**.** *Consider the double-integrator network* (1)*. Suppose that L is normal and the input $\mathbf{w}_0$ in* (5) *has unit covariance, i.e. $E[\Sigma_0]=I$. Then, the expectation of the performance metric P in* (4) *is*

$$E\left[P\right]=\|T\|_{\mathcal{H}_2}^2=\sum_{k\in\mathcal{N}_{obsv}}\nu_{kk}\frac{\phi_k}{2(\alpha_k\phi_k^2+\beta_k\xi_k\phi_k-\beta_k^2)},\quad(31)$$

for the position-based output, i.e. the system T given by (14a) *and*

$$E\left[P\right]=\|T\|_{\mathcal{H}_2}^2=\sum_{k\in\mathcal{N}_{obsv}}\nu_{kk}\frac{\xi_k\beta_k+\phi_k\alpha_k}{2(\alpha_k\phi_k^2+\beta_k\xi_k\phi_k-\beta_k^2)},\quad(32)$$

for the velocity-based output, i.e. the system T given by (14b)*; where $\alpha_k=k_p+\gamma_p\operatorname{Re}[\lambda_k]$, $\phi_k=k_d+\gamma_d\operatorname{Re}[\lambda_k]$, $\beta_k=\gamma_p\operatorname{Im}[\lambda_k]$ and $\xi_k=\gamma_d\operatorname{Im}[\lambda_k]$.*

Proof. See [38], [39] for a proof. □

Note that per Lemma 3 all ν_{kk} in (31) and (32) are positive. In addition, stability guarantees that the numerators and the denominators in (31) and (32) are positive due to Proposition 3. Therefore, the performance metrics are guaranteed to be positive quantities as expected.

In the next section, we study the effect of interconnection directionality on performance.

VI. The Role of Interconnection Directionality

In this section, we use the closed-form solutions from the previous section to investigate the effect of directionality. The class of graphs with normal weighted Laplacian matrices can for example arise in spatially invariant systems [6], [12], which are commonly used to model vehicle formations. Given any normal weighted Laplacian matrix L, we extract its Hermitian part as

$$L':=\frac{L+L^*}{2}.\quad(33)$$

Since L is weight-balanced [5, Lemma 4], (33) gives the Laplacian matrix of an undirected graph $\mathcal{G}'=\{\mathcal{N},\mathcal{E}',\mathcal{W}'\}$, where $\mathcal{E}'=\mathcal{E}\cup\{(j,i)\mid(i,j)\in\mathcal{E}\}$ and $\mathcal{W}'=\{\frac{b_{ij}+b_{ji}}{2}\mid b_{ij}\in\mathcal{W}\}$. In other words, $\mathcal{G}'$ is the *undirected counterpart* of $\mathcal{G}$ resulting from creating reverse edges in $\mathcal{G}$ and re-defining edge weights such that both graphs have the same nodal out-degree. Defining these two related graphs enables a comparison between an undirected vehicle formation and that with limited sensor placement (e.g. uni-directional measurements) or non-symmetric weighting of bi-directional measurements. Normality of L and (33) imply that the spectrum of L' has the property,

$$\operatorname{spec}(L')=\{\operatorname{Re}[\lambda_i]|\lambda_i\in\operatorname{spec}(L),i=1,\dots,n\}.\quad(34)$$

In addition, since L is normal, it has eigenvalues with non-zero imaginary parts if and only if its graph $\mathcal{G}$ is directed. For disturbance inputs that are uniform and uncorrelated across the network, we observe that both the position and velocity based performance metrics (31) and (32) depend on both the real and imaginary parts of the Laplacian eigenvalues. Therefore, comparison of directed graphs $\mathcal{G}$ and their undirected counterparts $\mathcal{G}'$ can reveal the interplay between the imaginary parts, i.e. edge directionality and control strategy (selection of control gains) that determines overall performance.

A. Position based Performance

We now provide a comparison of double-integrator systems with respective Laplacians L and L' for the position based performance metric (31).

Remark 4. *The performance metric in* (31) *simplifies to an expression that does not explicitly depend on $\operatorname{Im}[\lambda_k]$ if $\beta_k\xi_k\phi_k-\beta_k^2=0$ for all $k\in\mathcal{N}_{obsv}$. This condition holds if $\operatorname{Im}[\lambda_k]=0$ for all $k\in\mathcal{N}_{obsv}$, i.e. the effect of directed paths is not observed from the output, or L is symmetric, or $\gamma_p=0$, i.e. relative position feedback is absent. If $\beta_k\xi_k\phi_k-\beta_k^2=0$ for all $k\in\mathcal{N}_{obsv}$,* (31) *reduces to*

$$\|T\|_{\mathcal{H}_2}^2=\sum_{k\in\mathcal{N}_{obsv}}\nu_{kk}\frac{1}{2(k_p+\gamma_p\operatorname{Re}[\lambda_k])(k_d+\gamma_d\operatorname{Re}[\lambda_k])},\quad(35)$$

when the stability condition (21) *from Proposition 3 holds.*

The following Lemma shows the effect of the imaginary parts of the weighted Laplacian eigenvalues on the position based performance (31) of the double-integrator network (1).

Lemma 5 (Characterization of Position based Performance via the Observable Eigenvalues)**.** *Consider the double-integrator network* (1) *and the performance metric P in* (4)*. Let T and T' be the systems given by* (14a) *with weighted Laplacian matrices L and L'. Suppose L is normal and L' is given by* (33)*. Then the following hold:*

1) $\|T\|_{\mathcal{H}_2}^2=\|T'\|_{\mathcal{H}_2}^2$ *if* $\operatorname{Im}[\lambda_k]=0\ \forall k\in\mathcal{N}_{obsv}$.
2) $\|T\|_{\mathcal{H}_2}^2\le\|T'\|_{\mathcal{H}_2}^2$ *if*
$$\gamma_d(k_d+\gamma_d\operatorname{Re}[\lambda_k])-\gamma_p\ge0,\quad\forall k\in\mathcal{N}_{obsv}.\quad(36)$$
Furthermore, $\|T\|_{\mathcal{H}_2}^2<\|T'\|_{\mathcal{H}_2}^2$ if in addition at least one of the inequalities in (36) *strictly holds for some $k\in\mathcal{N}_{obsv}$ such that $\operatorname{Im}[\lambda_k]\neq0$ and relative position feedback is present, i.e. $\gamma_p>0$. Similarly, $\|T\|_{\mathcal{H}_2}^2\ge\|T'\|_{\mathcal{H}_2}^2$ if*
$$\gamma_d(k_d+\gamma_d\operatorname{Re}[\lambda_k])-\gamma_p\le0,\quad\forall k\in\mathcal{N}_{obsv}.\quad(37)$$
Furthermore, $\|T\|_{\mathcal{H}_2}^2>\|T'\|_{\mathcal{H}_2}^2$ if in addition at least one of the inequalities in (37) *strictly holds for some $k\in\mathcal{N}_{obsv}$ such that $\operatorname{Im}[\lambda_k]\neq0$ and relative position feedback is present, i.e. $\gamma_p>0$.*

Proof. Invoking Remark 4 and using (34), both $\|T\|_{\mathcal{H}_2}^2$ and $\|T'\|_{\mathcal{H}_2}^2$ are given by (35) which leads to Item *1)*. Condition (36) implies that $\beta_k\xi_k\phi_k-\beta_k^2\ge0$ for $k\in\mathcal{N}_{obsv}$ therefore

$$\frac{\phi_k}{2(\alpha_k\phi_k^2+\beta_k\xi_k\phi_k-\beta_k^2)}\le\frac{1}{2\alpha_k\phi_k},\quad k\in\mathcal{N}_{obsv}.\quad(38)$$

Since $\nu_{kk}>0$ for $k\in\mathcal{N}_{obsv}$ due to Lemma 3, multiplication of both sides of (38) by ν_{kk} and summation of the inequalities gives $\|T\|_{\mathcal{H}_2}^2\le\|T'\|_{\mathcal{H}_2}^2$. If in addition to (36) at least one of these inequalities strictly holds for some $k\in\mathcal{N}_{obsv}$ such that $\operatorname{Im}[\lambda_k]\neq0$ and $\gamma_p>0$, then $\|T\|_{\mathcal{H}_2}^2<\|T'\|_{\mathcal{H}_2}^2$. The reverse inequalities follow from (37) using similar arguments. □

Remark 5. *Note that the results in Lemma 5 hold for any output matrix C satisfying Assumption 3. The terms ν_{kk} contain parameters that depend on C as given in* (25)*. Since the Laplacians L and L' share their eigenspace, these terms are common in their respective performance metrics.*

It is necessary that at least one observable eigenvalue does not lie on the real line for the performance of the directed and undirected systems to differ, and the gains need to be tuned based on these eigenvalues to improve performance. We next use this result to characterize the position-based performance of directed and undirected double-integrator systems in terms of relative feedback.

Theorem 2 (Characterization of Position based Performance via Relative Feedback)**.** *Consider the double-integrator network* (1) *and the performance metric* P *in* (4)*. Let* T *and* T' *be the systems given by* (14a) *with weighted Laplacian matrices* L *and* L'*. Suppose that* L *is normal and* L' *is given by* (33)*. Then the following hold:*

1) *If relative position feedback is absent, i.e.* $\gamma_p = 0$*, then* $\|T\|^2_{\mathcal{H}_2} = \|T'\|^2_{\mathcal{H}_2}$.
2) *If relative position feedback is present and relative velocity feedback is absent, i.e.* $\gamma_p > 0$ *and* $\gamma_d = 0$*, and* $\mathrm{Im}[\lambda_k] \neq 0$ *for some* $k \in \mathcal{N}_{obsv}$*, then* $\|T\|^2_{\mathcal{H}_2} > \|T'\|^2_{\mathcal{H}_2}$.
3) *If both relative position and velocity feedback are present, i.e.* $\gamma_p > 0$ *and* $\gamma_d > 0$*, and* $\mathrm{Im}[\lambda_k] \neq 0$ *for some* $k \in \mathcal{N}_{obsv}$*, then there exists* $\underline{\gamma}_p$ *and* $\overline{\gamma}_p$ *that satisfy*

$$\min_{\substack{k\in\mathcal{N}_{obsv},\\ \mathrm{Im}[\lambda_k]\neq 0}} \mathrm{Re}[\lambda_k] \leq \frac{\underline{\gamma}_p}{\gamma_d^2} - \frac{k_d}{\gamma_d} \leq \frac{\overline{\gamma}_p}{\gamma_d^2} - \frac{k_d}{\gamma_d} \leq \max_{\substack{k\in\mathcal{N}_{obsv},\\ \mathrm{Im}[\lambda_k]\neq 0}} \mathrm{Re}[\lambda_k],$$

such that $\|T\|^2_{\mathcal{H}_2} < \|T'\|^2_{\mathcal{H}_2}$ *if* $\gamma_p < \underline{\gamma}_p$ *and* $\|T\|^2_{\mathcal{H}_2} > \|T'\|^2_{\mathcal{H}_2}$ *if* $\gamma_p > \overline{\gamma}_p$.

Proof. Invoking Remark 4 and using (34) leads to Item *1)*. Item *2)* follows from Lemma 5 by setting $\gamma_p > 0$ and $\gamma_d = 0$ in (37). To prove Item *3)* we observe from Lemma 5 that

$$\gamma_p > \max_{\substack{k\in\mathcal{N}_{obsv},\\ \mathrm{Im}[\lambda_k]\neq 0}} \gamma_d(k_d + \gamma_d \mathrm{Re}[\lambda_k]) =: \gamma_u \Rightarrow \|T\|^2_{\mathcal{H}_2} > \|T'\|^2_{\mathcal{H}_2},$$

$$\gamma_p < \min_{\substack{k\in\mathcal{N}_{obsv},\\ \mathrm{Im}[\lambda_k]\neq 0}} \gamma_d(k_d + \gamma_d \mathrm{Re}[\lambda_k]) =: \gamma_l \Rightarrow \|T\|^2_{\mathcal{H}_2} < \|T'\|^2_{\mathcal{H}_2}.$$

So $\|T\|^2_{\mathcal{H}_2} = \|T'\|^2_{\mathcal{H}_2}$ if $\gamma_p = \underline{\gamma}_p$ and $\|T\|^2_{\mathcal{H}_2} < \|T'\|^2_{\mathcal{H}_2}$ if $\gamma_p < \underline{\gamma}_p$ for some $\underline{\gamma}_p \in [\gamma_l, \gamma_u]$, since $\|T\|^2_{\mathcal{H}_2}$ and $\|T'\|^2_{\mathcal{H}_2}$ are continuous in γ_p. Similarly, $\|T\|^2_{\mathcal{H}_2} = \|T'\|^2_{\mathcal{H}_2}$ if $\gamma_p = \overline{\gamma}_p$ and $\|T\|^2_{\mathcal{H}_2} > \|T'\|^2_{\mathcal{H}_2}$ if $\gamma_p > \overline{\gamma}_p$ for some $\overline{\gamma}_p \in [\gamma_l, \gamma_u]$. Finally we note that $\underline{\gamma}_p \leq \overline{\gamma}_p$, because otherwise $\gamma_p = \underline{\gamma}_p > \overline{\gamma}_p$ would imply that $\|T\|^2_{\mathcal{H}_2} = \|T'\|^2_{\mathcal{H}_2}$ and $\|T\|^2_{\mathcal{H}_2} > \|T'\|^2_{\mathcal{H}_2}$ must simultaneously hold, which is a contradiction. □

Directionality degrades performance for metrics that capture some of the modes resulting from the directed paths (i.e. $\mathrm{Im}[\lambda_k] \neq 0$ for some $k \in \mathcal{N}_{obsv}$) if relative position feedback is used without relative velocity feedback. This degradation can be addressed in several ways depending on the available feedback. For example, omitting relative position feedback (which requires absolute position feedback due to Assumption 2) can mitigate this degradation. In this case, the directionality of relative velocity feedback does not affect performance as directed and undirected systems perform identically.

When both types of relative feedback are used, tuning their respective gains properly can, not only mitigate the performance degradation, but also lead to the directed system outperforming its undirected counterpart. Therefore, it is critical to have relative velocity feedback in addition to relative position feedback. In other words, the directed system performs better than its undirected counterpart for sufficiently small relative position gain (the converse is true for sufficiently large relative position gain). This sufficient magnitude is determined by the velocity gains as well as the magnitude of the real parts of the observable eigenvalues that have non-zero imaginary parts. As a consequence, a judicious control strategy depends on the topological characteristics of the network.

B. Velocity based Performance

This subsection provides a comparison of the double integrator systems with respective Laplacians L and L' in terms of the velocity based performance metric given in (32).

Remark 6. *The performance metric in* (32) *simplifies to an expression that does not explicitly depend on* $\mathrm{Im}[\lambda_k]$ *if* $\beta_k = 0$ *for all* $k \in \mathcal{N}_{obsv}$*. This condition holds if* $\mathrm{Im}[\lambda_k] = 0$ *for all* $k \in \mathcal{N}_{obsv}$*, i.e. the effect of directed paths is not observed from the output, or* L *is symmetric, or* $\gamma_p = 0$*, i.e. relative position feedback is absent. If* $\beta_k = 0$ *for all* $k \in \mathcal{N}_{obsv}$*,* (32) *reduces to*

$$\|T\|^2_{\mathcal{H}_2} = \sum_{k\in\mathcal{N}_{obsv}} \nu_{kk} \frac{1}{2(k_d + \gamma_d \mathrm{Re}[\lambda_k])}, \tag{39}$$

when the stability condition (21) *from Proposition 3 holds.*

In contrast to the position based performance metric in (35), the velocity based performance in (39) depends only on the absolute or relative velocity feedback and its denominator is affine in $\mathrm{Re}[\lambda_k]$. So, absolute or relative position feedback does not affect velocity based performance if $\mathcal{G}$ is undirected.

The following theorem demonstrates that if the velocity based performance of the system given by (14b) is considered and its directed graph emits a normal weighted Laplacian, its $\mathcal{H}_2$ norm is lower bounded by the $\mathcal{H}_2$ norm of the corresponding undirected system whose interconnection is defined by (33). This result highlights the inability of standard feedback schemes to mitigate velocity-based performance degradation caused by directionality.

Theorem 3 (Characterization of Velocity based Performance)**.** *Consider the double-integrator network* (1) *and the performance metric* P *in* (4)*. Let* T *and* T' *be the systems given by* (14b) *with weighted Laplacian matrices* L *and* L'*. Suppose that* L *is normal and* L' *is given by* (33)*. Then the following hold:*

1) $\|T\|^2_{\mathcal{H}_2} \geq \|T'\|^2_{\mathcal{H}_2}$.
2) $\|T\|^2_{\mathcal{H}_2} > \|T'\|^2_{\mathcal{H}_2}$ *if and only if* $\mathrm{Im}[\lambda_k] \neq 0$ *for some* $k \in \mathcal{N}_{obsv}$ *and relative position feedback is present, i.e.* $\gamma_p > 0$.
3) $\|T\|^2_{\mathcal{H}_2} = \|T'\|^2_{\mathcal{H}_2}$ *if and only if* $\mathrm{Im}[\lambda_k] = 0\ \forall k \in \mathcal{N}_{obsv}$ *or relative position feedback is absent, i.e.* $\gamma_p = 0$.

Proof. Since $-\beta_k^2 = -\gamma_p^2 \mathrm{Im}[\lambda_k]^2 \leq 0$, it holds that

$$\alpha_k\phi_k^2 + \beta_k\xi_k\phi_k - \beta_k^2 \leq \alpha_k\phi_k^2 + \beta_k\xi_k\phi_k, \quad k \in \mathcal{N}_{obsv}. \tag{40}$$

Stability condition (21) from Proposition 3 states that

$$\alpha_k\phi_k^2 + \beta_k\xi_k\phi_k - \beta_k^2 > 0 \text{ and } \phi_k > 0, \quad k \in \mathcal{N}_{obsv}. \tag{41}$$

Therefore, (40) can be re-arranged as

$$\frac{\xi_k\beta_k + \phi_k\alpha_k}{\alpha_k\phi_k^2 + \beta_k\xi_k\phi_k - \beta_k^2} \geq \frac{1}{\phi_k}, \quad k \in \mathcal{N}_{obsv}. \tag{42}$$

Since $\nu_{kk} > 0$ for $k \in \mathcal{N}_{obsv}$ as shown in Lemma 3,

$$\nu_{kk}\frac{\xi_k\beta_k + \phi_k\alpha_k}{2(\alpha_k\phi_k^2 + \beta_k\xi_k\phi_k - \beta_k^2)} \geq \nu_{kk}\frac{1}{2\phi_k}, \quad k \in \mathcal{N}_{obsv}. \tag{43}$$

Summation of the inequalities given in (43) and using (32) and (39) leads to Item *1)*.

To prove the necessity part of Item *2)*, we observe that $-\beta_k^2 = -\gamma_p^2 \mathrm{Im}[\lambda_k]^2 < 0$ for some $k \in \mathcal{N}_{obsv}$ therefore (40) strictly holds for such k. Then by a similar argument to the one used to prove Item *1)*, (43) strictly holds for such k as well, which leads to $\|T\|^2_{\mathcal{H}_2} > \|T'\|^2_{\mathcal{H}_2}$. To prove sufficiency suppose that $\|T\|^2_{\mathcal{H}_2} > \|T'\|^2_{\mathcal{H}_2}$. Using (32) and (39), this inequality implies that (43) strictly holds for some $k \in \mathcal{N}_{obsv}$ (otherwise $\|T\|^2_{\mathcal{H}_2} = \|T'\|^2_{\mathcal{H}_2}$). Since $\nu_{kk} > 0$ for $k \in \mathcal{N}_{obsv}$, (42) strictly holds for some $k \in \mathcal{N}_{obsv}$ as well. Using (41) and re-arranging terms leads to $\beta_k^2 = \gamma_p^2 \mathrm{Im}[\lambda_k]^2 > 0$ for some $k \in \mathcal{N}_{obsv}$ implying that $\mathrm{Im}[\lambda_k] \neq 0$ for some $k \in \mathcal{N}_{obsv}$ and $\gamma_p > 0$. Finally we note that items *1)* and *2)* imply Item *3)*. □

Unlike position based performance, there does not exist a choice of control gains for the directed system that gives better velocity based performance compared to its undirected counterpart for any output matrix C satisfying Assumption 3. Furthermore, when relative position feedback is used, the directed system performs strictly worse compared to its undirected counterpart under metrics capturing the effect of the directed interconnection. They perform identically without relative position feedback or if metrics do not capture directionality.

When the overall system performance is considered in terms of both position and velocity based metrics, a trade-off emerges. For systems with observable directed paths, it is possible to have performance equal to that of their undirected counterparts for both position and velocity based metrics by omitting relative position feedback. But this is true only if absolute position feedback is used, as it is required for stability (Assumption 2). Therefore, unless absolute position measurements are available, the directed system requires well-tuned gains to prevent degradation of the position-based performance (or to possibly improve it), while it will always have worse velocity-based performance compared to the undirected system. For directed systems with absolute position feedback, improving position-based performance comes at the expense of the velocity-based performance.

Remark 7. *For the metric defined as the variance of the full-state, the $\mathcal{H}_2$ norm of a linear system can be upper bounded by the $\mathcal{H}_2$ norm of a system whose dynamics emit the Hermitian part of the original state matrix [33, Theorem 2]. In the case of double-integrator networks, this comparison does not explicitly account for the Laplacian eigenvalues, i.e. interconnection directionality. In contrast, we characterized the role of directionality in general quadratic metrics by identifying the interplay between complex Laplacian eigenvalues and the control strategy. This interplay also contrasts the equivalence of effective graph resistance between directed cycle and path graphs and their respective undirected counterparts [36, Proposition 1].*

Remark 8. *Scaling properties of network performance with respect to network size and graph structure have been investigated, see e.g. [6], [12], [31], [40]. Normal Laplacian matrices can represent some of these graph structures, including regular graphs (spatially invariant formations in multiple dimensions). Our closed-form solutions provide generalizations of those previously reported for this class of network topologies [6], [12], [31] by addressing the case of general quadratic performance metrics. Our analysis also complements the scaling properties established for large-scale networks by demonstrating the role of directionality when the network size is a fixed parameter.*

Remark 9. *A subclass of directed graphs emitting normal Laplacians can destabilize integrator networks of sufficiently large size unless absolute feedback of certain states is deployed [31], [41]. For this subclass of directed graphs, we consider cases ensuring stability through either appropriate absolute feedback or allowable network size that is determined by network topology and control gains.*

C. Example: Position and Velocity based Performance with Uni-directional vs. Bi-directional Feedback

We now consider a cyclic digraph in which each node has uniform out-degree d and the uniformly weighted edges that start at each node reach ω succeeding nodes. This results in 'look-ahead' type state measurements through ω communication hops. The respective weighted Laplacian is given by

$$L^{cyc}(d,\omega)=d\times\mathrm{circ}\left(\begin{bmatrix}1 & -\frac{1}{\omega} & \dots & -\frac{1}{\omega} & 0 & \dots & 0\end{bmatrix}\right), \quad (44)$$

where $d\in\mathbb{R}^+$, $\omega\in\mathbb{Z}^+$, $\omega\leq n-1$ and $\mathrm{circ}(\cdot)$ denotes the circulant matrix generated by permuting the row vector in the argument. The Jordan decomposition of $L=L^{cyc}$ gives [42]

$$J_k=\lambda_k=d\left(1-\frac{1}{\omega}\sum_{i=1}^{\omega}e^{-\mathbf{j}\frac{2\pi}{n}i(k-1)}\right), \quad (45)$$

for $k=1,\dots,n$. Choosing $\alpha=\frac{1}{\sqrt{n}}$ in (15), the columns of $\tilde{R}$ are

$$\mathbf{r}_l=\frac{1}{\sqrt{n}}\begin{bmatrix}1 & e^{\mathbf{j}\frac{2\pi}{n}(l-1)} & \dots & e^{\mathbf{j}\frac{2\pi}{n}(l-1)(n-1)}\end{bmatrix}^*, \quad (46)$$

for $l=2,\dots,n$. For the special case of uni-directional feedback, we set $d=1$ and $\omega=1$ in (44) therefore

$$L=L^{cyc}(1,1)\quad\text{and}\quad L'=\frac{L^{cyc}(1,1)+L^{cyc}(1,1)^*}{2},$$

where we have used (33) to also define the corresponding bi-directional feedback. We consider the respective systems T and T' with an arbitrary output matrix $C\in\mathbb{R}^{n\times n}$ that satisfies Assumption 3, for $n=50$.

For the double-integrator network (1) given by (14a) (position based performance), Figure 4a shows that, using relative position feedback without relative velocity feedback ($\gamma_p>0$ and $\gamma_d=0$) leads to worse performance with directed interconnection, in accordance with Item *2)* of Theorem 2. It is when both relative position and velocity measurements are used ($\gamma_p>0$ and $\gamma_d>0$) that the directed cycles can be utilized to attain better performance by tuning the gains. Per Item *3)* of Theorem 2, sufficiently small γ_p (i.e. sufficiently large velocity gains k_d and γ_d) improves the performance of the directed interconnection relative to its undirected counterpart; but the performance degrades for sufficiently large γ_p, as shown in Figure 4b. Directed cycles require less communication and thus can be preferable, provided the gains are carefully selected.

For the double-integrator network (1) given by (14b) (velocity based performance), Figure 4c shows that relative position feedback degrades performance if the cycles are directed. But the performance is comparable to that of the undirected system for sufficiently small γ_p, equaling it at $\gamma_p=0$. This supports the results of Theorem 3.

VII. Conclusion

We developed an analysis framework to compute general quadratic performance metrics for integrator networks defined over arbitrary directed graphs that have at least one globally reachable node. We used this framework to study the class of directed graphs with normal weighted Laplacians. The analysis reveals the importance of well-designed feedback for mitigating any performance degradation in double-integrator networks with this class of directed graphs; and the potential for exploiting directed feedback to improve performance over that of its undirected counterpart. Our framework can be used to obtain further insights into the effect of topological characteristics on network performance, see [38], [39] for other applications.

References

[1] W. Ren and E. Atkins, "Second-order consensus protocols in multiple vehicle systems with local interactions," in *AIAA Guidance, Navigation, and Control Conf. and Exhibit*, Aug. 2005, pp. 6238–6251.

[2] W. Yu, G. Chen, and M. Cao, "Some necessary and sufficient conditions for second-order consensus in multi-agent dynamical systems," *Automatica*, vol. 46, no. 6, pp. 1089–1095, 2010.

[3] J. Zhu, Y. Tian, and J. Kuang, "On the general consensus protocol of multi-agent systems with double-integrator dynamics," *Linear Algebra Appl.*, vol. 431, no. 5, pp. 701–715, 2009.

[4] M. Siami and N. Motee, "Fundamental limits and tradeoffs on disturbance propagation in linear dynamical networks," *IEEE Trans. Autom. Control*, vol. 61, no. 12, pp. 4055–4062, Dec. 2016.

[5] G. F. Young, L. Scardovi, and N. E. Leonard, "Robustness of noisy consensus dynamics with directed communication," in *Proc. of the American Ctrl. Conf.*, Jun. 2010, pp. 6312–6317.

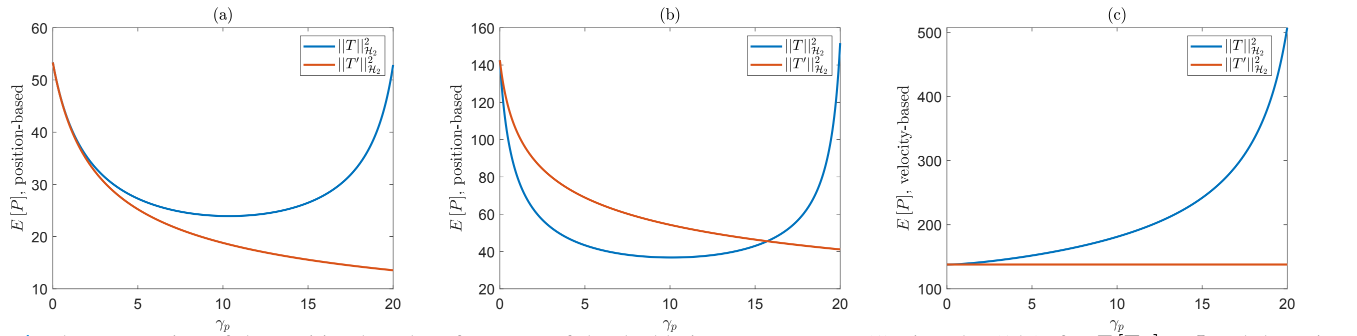

Fig. 4: The expectation of the position-based performance of the double-integrator system (1) given by (14a), for $E[\Sigma_0] = I$ and the gains **(a)** $k_p = 3, k_d = 5, \gamma_d = 0$, **(b)** $k_p = 1, k_d = 2, \gamma_d = 6.5$. **(c)** The expectation of the velocity-based performance of the double-integrator system (1) given by (14b), for $E[\Sigma_0] = I$ and the gains $k_p = 1, k_d = 2, \gamma_d = 7$.

[6] B. Bamieh, M. R. Jovanović, P. Mitra, and S. Patterson, “Coherence in large-scale networks: Dimension-dependent limitations of local feedback,” *IEEE Trans. on Autom. Ctrl.*, vol. 57, no. 9, pp. 2235–2249, Sep. 2012.

[7] S. Dezfulian, Y. Ghaedsharaf, and N. Motee, “On performance of time-delay linear consensus networks with directed interconnection topologies,” in *Proc. of the American Ctrl. Conf.*, Jun. 2018.

[8] T. Sarkar, M. Roozbehani, and M. A. Dahleh, “Asymptotic robustness in consensus networks,” in *2018 Annual American Ctrl. Conf. (ACC)*, June 2018, pp. 6212–6217.

[9] X. Ma and N. Elia, “Mean square performance and robust yet fragile nature of torus networked average consensus,” *IEEE Trans. on Ctrl. of Network Systems*, vol. 2, no. 3, pp. 216–225, Sep. 2015.

[10] F. Lin, M. Fardad, and M. R. Jovanović, “Performance of leader-follower networks in directed trees and lattices,” in *in Proc. of the 51st IEEE Conf. on Dec. and Ctrl.*, Dec. 2012, pp. 734–739.

[11] T. W. Grunberg and D. F. Gayme, “Performance measures for linear oscillator networks over arbitrary graphs,” *IEEE Trans. on Ctrl. of Network Systems*, vol. 5, no. 1, pp. 456–468, Mar. 2018.

[12] E. Tegling, P. Mitra, H. Sandberg, and B. Bamieh, “On fundamental limitations of dynamic feedback control in regular large-scale networks,” *IEEE Trans. on Autom. Ctrl.*, vol. 64, no. 12, pp. 4936–4951, 2019.

[13] R. Pates, C. Lidström, and A. Rantzer, “Control using local distance measurements cannot prevent incoherence in platoons,” in *In Proc. of the 56th IEEE Conf. on Dec. and Ctrl.*, Dec. 2017, pp. 3461–3466.

[14] H. Hao and P. Barooah, “Stability and robustness of large platoons of vehicles with double-integrator models and nearest neighbor interaction,” *International Journal of Robust and Nonlinear Control*, vol. 23, no. 18, pp. 2097–2122, Dec. 2013.

[15] F. Lin, M. Fardad, and M. R. Jovanović, “Optimal control of vehicular formations with nearest neighbor interactions,” *IEEE Trans. Autom. Control*, vol. 57, no. 9, pp. 2203–2218, Sep. 2012.

[16] H. G. Oral, E. Mallada, and D. F. Gayme, “Performance of first and second order linear networked systems over digraphs,” in *Proc. of the 56th IEEE Conf. on Dec. and Ctrl.*, Dec. 2017, pp. 1688–1694.

[17] B. Bamieh and D. F. Gayme, “The price of synchrony: Resistive losses due to phase synchronization in power networks,” in *Proc. of the American Ctrl. Conf.*, Jun. 2013, pp. 5815–5820.

[18] E. Tegling, B. Bamieh, and D. F. Gayme, “The price of synchrony: Evaluating the resistive losses in synchronizing power networks,” *IEEE Trans. on Ctrl. of Network Sys.*, vol. 2, no. 3, pp. 254–266, Sep. 2015.

[19] E. Tegling, D. F. Gayme, and H. Sandberg, “Performance metrics for droop-controlled microgrids with variable voltage dynamics,” in *Proc. of the 54th IEEE Conf. on Dec. and Ctrl.*, Dec. 2015, pp. 7502–7509.

[20] E. Mallada, “iDroop: A dynamic droop controller to decouple power grid’s steady-state and dynamic performance,” in *55th IEEE Conf. on Dec. and Ctrl. (CDC)*, Dec. 2016, pp. 4957–4964.

[21] Y. Jiang, R. Pates, and E. Mallada, “Performance tradeoffs of dynamically controlled grid-connected inverters in low inertia power systems,” in *56th IEEE Conf. on Dec. and Ctrl. (CDC)*, Dec. 2017, pp. 5098–5105.

[22] E. Weitenberg, Y. Jiang, C. Zhao, E. Mallada, C. De Persis, and F. Dörfler, “Robust decentralized secondary frequency control in power systems: Merits and trade-offs,” *IEEE Trans. on Autom. Ctrl.*, Dec. 2018, doi: 10.1109/TAC.2018.2884650.

[23] X. Wu, F. Dörfler, and M. R. Jovanović, “Input-output analysis and decentralized optimal control of inter-area oscillations in power systems,” *IEEE Trans. on Power Sys.*, vol. 31, no. 3, pp. 2434–2444, May 2016.

[24] J. W. Simpson-Porco, B. K. Poolla, N. Monshizadeh, and F. Dörfler, “Quadratic performance of primal-dual methods with application to secondary frequency control of power systems,” in *2016 IEEE 55th Conf. on Dec. and Ctrl. (CDC)*, Dec 2016, pp. 1840–1845.

[25] H. G. Oral and D. F. Gayme, “Performance of droop-controlled microgrids with heterogeneous inverter ratings,” in *Proc. of the European Ctrl. Conf.*, Jun. 2019, pp. 1398–1405.

[26] M. Tyloo and P. Jacquod, “Global robustness versus local vulnerabilities in complex synchronous networks,” *Phys. Rev. E*, vol. 100, p. 032303, Sep. 2019.

[27] S. Patterson, Y. Yi, and Z. Zhang, “A resistance-distance-based approach for optimal leader selection in noisy consensus networks,” *IEEE Trans. on Ctrl. of Network Sys.*, vol. 6, no. 1, pp. 191–201, March 2019.

[28] F. Paganini and E. Mallada, “Global performance metrics for synchronization of heterogeneously rated power systems: The role of machine models and inertia,” in *55th Annual Allerton Conference on Communication, Control, and Computing (Allerton)*, Oct 2017, pp. 324–331.

[29] ——, “Global analysis of synchronization performance for power systems: Bridging the theory-practice gap,” *IEEE Trans. on Autom. Ctrl.*, vol. 65, no. 7, pp. 3007–3022, 2020.

[30] T. Coletta and P. Jacquod, “Performance measures in electric power networks under line contingencies,” *IEEE Trans. on Ctrl. of Network Systems*, vol. 7, no. 1, pp. 221–231, 2020.

[31] H. G. Oral and D. F. Gayme, “Disorder in large-scale networks with uni-directional feedback,” in *Proc. of the American Ctrl. Conf.*, Jul. 2019, pp. 3394–3401.

[32] C. Ji, E. Mallada, and D. F. Gayme, “Evaluating robustness of consensus algorithms under measurement error over digraphs,” in *2018 IEEE Conf. on Dec. and Ctrl. (CDC)*, Dec 2018, pp. 1238–1244.

[33] M. Siami and N. Motee, “New spectral bounds on h2-norm of linear dynamical networks,” *Automatica*, vol. 80, pp. 305–312, Jun. 2017.

[34] W. Ellens, F. M. Spieksma, P. V. Mieghem, A. Jamakovic, and R. E. Kooij, “Effective graph resistance,” *Linear Algebra Appl.*, vol. 435, no. 10, pp. 2491–2506, Nov. 2011.

[35] G. F. Young, L. Scardovi, and N. E. Leonard, “A new notion of effective resistance for directed graphs– part i: Definition and properties,” *IEEE Trans. Autom. Control*, vol. 61, no. 7, pp. 1727–1736, Jul. 2016.

[36] ——, “A new notion of effective resistance for directed graphs– part ii: Computing resistances,” *IEEE Trans. Autom. Control*, vol. 61, no. 7, pp. 1737–1752, Jul. 2016.

[37] F. Bullo, “Lectures on network systems,” *Online at http://motion.me.ucsb.edu/book-lns, with contributions by J. Cortes, F. Dörfler and S. Martinez*, 2016.

[38] H. G. Oral, E. Mallada, and D. F. Gayme, “Performance of single and double-integrator networks over directed graphs,” *arXiv preprint*, Nov. 2019, arXiv:1911.00791.

[39] H. G. Oral, “A characterization of network performance: The role of communication directionality and system heterogeneity,” *Ph.D. dissertation, Johns Hopkins University*, Aug. 2020.

[40] P. Barooah and J. P. Hespanha, “Error scaling laws for linear optimal estimation from relative measurements,” *IEEE Trans. on Information Theory*, vol. 55, no. 12, pp. 5661–5673, 2009.

[41] E. Tegling, B. Bamieh, and H. Sandberg, “Localized high-order consensus destabilizes large-scale networks,” in *2019 American Ctrl. Conf. (ACC)*, 2019, pp. 760–765.

[42] R. A. Horn and C. R. Johnson, *Matrix Analysis*. Cambridge University Press, 2012.